

SONEL MAPPING: ACOUSTIC MODELING UTILIZING AN ACOUSTIC VERSION OF PHOTON MAPPING

B. Kapralos^{1,3,4}, M. Jenkin^{1,3,4} and E. Milios^{2,3}

¹ Computer Science and Engineering, York University, Toronto, Ontario, Canada. M3J 1P3

² Faculty of Computer Science, Dalhousie University, Halifax, Nova Scotia, Canada. B3H 1W5

³ Centre for Vision Research, York University, Toronto, Ontario, Canada. M3J 1P3

⁴ Centre for Research in Space Technology (CRESTech), Toronto, Ontario, Canada. M3J 3K1

{billk, jenkin}@cs.yorku.ca

eem@cs.dal.ca

ABSTRACT

Acoustic modeling of even small simple environments is a complex, computationally expensive task. Sound, just as light, is itself a wave phenomenon. Although there are several key differences between light and sound there are also several similarities. Given the similarities which exist between sound and light, this work investigates the application of photon mapping (suitably modified), to model environmental acoustics. The resulting acoustic *sonel mapping* technique can be used to model acoustic environments while accounting for diffuse and specular acoustic reflections as well as refraction and diffraction effects.

1: INTRODUCTION

Incorporating spatialized auditory cues in an immersive virtual environment can be beneficial for a variety of reasons; spatial auditory cues can add a better sense of “presence” or “immersion”, they can compensate for poor visual cues (graphics), lead to improved object localization and at the very least, add a “pleasing quality” to the simulation [21]. Despite these potential benefits, spatial auditory cues are often overlooked in immersive virtual environments where traditionally emphasis has been placed on the visual (graphic) scenes [6]. Systems that do convey auditory information often do so poorly, typically assuming that all interactions (reflections) between a sound wave and objects/surfaces in the environment are specular, despite that in our natural settings, acoustical reflections may include diffuse, diffractive and refracted components as well. Failure to accurately model all the reflection phenomena (in particular, diffractive [23] and diffuse [14] components) leads to a decrease in the spatialization capabilities of the system, ultimately leading to a decrease in performance.

Given the importance of simulating the acoustics of an environment accurately and the similarities that exist between computer graphics and acoustic modeling, this work

investigates the application of photon mapping-like techniques (see [8] for a review of photon mapping) to model the acoustics of a dynamic environment. By accounting for the differences between the propagation of sound and light as well as how propagating sound waves interact when they encounter objects in the environment, a novel technique, termed *sonel mapping*, is developed that can be used to accurately model the acoustics of an environment.

This paper is organized as follows: Section 2 provides a brief introduction to auralization and describes some relevant room acoustic modeling techniques. A description of the sonel mapping method is described in Section 3, beginning with a brief description of the computer graphics based photon mapping method on which it is based. Test results are provided in Section 4 while a summary and discussion of future work is presented in Section 5.

2: AURALIZATION

The goal of auralization [9] is to recreate a particular listening environment, taking into account the acoustics of the environment (e.g., reverberation) and the characteristics of the listener (e.g., head related transfer functions or HRTFs). Auralization can be accomplished by determining the *bin-aural room impulse response* (BRIR). The BRIR can then be used to filter, typically through convolution, the desired sound material and when this filtered sound is presented to a listener, the original sound environment will be recreated. The BRIR can be decomposed into two separate components; i) the *room impulse response* (RIR) which captures the reflection properties (reverberation), sound attenuation and absorption properties of a particular room configuration (e.g., the “room acoustics”) and ii) the HRTF that captures the effects introduced by the listener, due to the listener’s physical make-up (e.g., pinnae, head, neck, torso). Greater detail regarding the determination of the HRTF, in addition to human sound localization in general, is provided in [3]

and will not be described further here.

2.1: Estimating the Room Impulse Response

Current approaches to computational acoustic modeling can be broadly divided into two categories; *wave-based modeling* and *ray based modeling* [18]¹.

Wave-Based Methods: With wave-based methods, the objective is to solve the wave equation, also known as the *Helmholtz* equation, to recreate a particular sound field. Unfortunately, an analytical solution to the *wave equation* is rarely feasible [18] and wave-based methods use numerical approximations, such as finite element methods (FEM), boundary element methods (BEM) and finite difference time domain methods (FDTD) instead [18]. With respect to acoustical wave-based methods, numerical approximations sub-divide the boundaries of a room into smaller elements. Then, by assuming the pressure at each of these elements is a linear combination of a finite number of basis functions, the “boundary integral form” of the wave equation can be solved [6]. An example of such an approach is the acoustical radiosity method [16, 20], which is itself a modified version of the image synthesis radiosity technique.

Geometric Acoustics and Ray-Based Techniques: In a manner similar to geometric optics, ray based acoustical modeling, assumes sound acts as rays. Hence, light (visual) based rendering techniques are used to model the acoustics of an environment. Essentially, the propagation paths taken by the rays are found by tracing (following) these “acoustic rays”. Mathematical models are used to account for source emission patterns, atmospheric scattering, absorption of the sound ray by the medium itself and the interactions with any surfaces/objects the rays may encounter [6]. At the receiver, the RIR is obtained by constructing an *echogram*, describing the distribution of incident sound energy (rays) over time. Several of the more popular ray-based methods include *image sources* [1], *ray tracing* [10] and *beam tracing* [5].

The numerical approximations associated with wave based methods are computationally very expensive, making them impractical for all but very simple, static environments. Furthermore, their computational complexity increases linearly with the volume of the room and the number of volume elements and is proportional to the fourth power of the frequency of interest [17]. Such techniques are currently beyond our computational ability for all but very simple, trivial scenarios.

Ray based methods, on the other hand, are fairly simple to model and are widely used in a variety of acoustical modeling applications. Unfortunately, they are only valid

for higher frequency sounds, where reflections are typically specular. Ray based methods thus ignore the wavelength of sound and phenomena associated with diffraction. By ignoring such phenomena, they can only accurately model the early portion of the room impulse response as these techniques become computationally expensive as the number of reflections increases [6]. Ray based methods also fail to properly account for diffuse reflections, leading to higher predicted reverberation times [7] and generally, a decrease in the overall quality of the auralization [13]. Models that do attempt to account for diffuse reflections, according to Dalenbäck et al. [14], do so in a “crude manner”.

3: SONEL MAPPING

In this paper we propose a novel technique for auralization called *sonel mapping*. Sonel mapping is an application of the photon mapping computer graphics method to auralization. Photon mapping [8] is a two-pass “particle-based”, probabilistic global illumination method developed by Jensen in 1995 in order to determine the illumination at any point in a scene. In the first pass, “photons” (the basic quantity of light) are emitted from each light source and traced through the scene until they interact with a surface. When photons encounter a diffuse surface, they are stored in a structure called a *photon map*. In the second stage, the scene is rendered using the information provided by the previously collected photon map to provide a quick estimate of the diffuse reflected illumination. Distribution ray tracing is employed to model specular effects. Photon mapping is independent of the scene geometry, thereby allowing for the illumination of arbitrary complex scenes to be computed. In addition, it can handle complex interactions between light and a surface, including pure specular, pure diffuse and glossy reflections and any combination of them.

Here we use the same basic approach as photon mapping but apply the technique to the task of auralization. Consider the possible outcomes when a propagating sound encounters a surface/object or obstruction in its path (see Figure 1). A propagating sound can experience specular or diffuse reflection, refraction, diffraction or absorption, solely or in any combination. Following the same strategy as used in photon mapping, rather than modeling the exact *mechanical wave* phenomena of sound propagation (e.g., particles in the medium as they move about in their equilibrium position), at each source, this process is approximated by emitting one or more “sound elements” (the analogue to photons when considering the visual photon mapping method), from the sound source and tracing these sound elements through the scene until they encounter an object/surface. (Hereinafter, a sound element will be referred to as a *sonel* or *sonels* when considering more than one sound element). The sonel can be viewed as a packet

¹Actually, Savioja [18] includes a third category called *statistical modeling*. As described in [18], statistical modeling is primarily applied to “predict noise levels in coupled systems in which sound transmission by structures is an important factor” and hence not suitable for auralization.

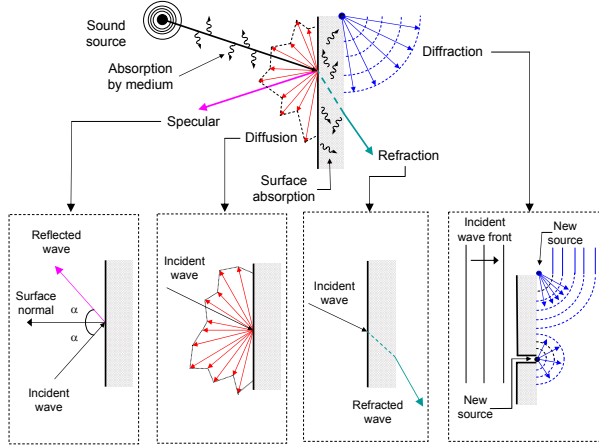


Fig. 1. Acoustic reflection phenomena.

of information propagating from the sound source to the receiver, carrying the relevant information required to simulate the mechanical wave propagation. The information carried by each sonel includes the information used by photons in the photon mapping approach: position (x,y,z coordinates), direction to incidence and energy in addition to information specific to sound and sound propagation, including: distance traveled, phase and frequency.

The goal of sonel mapping is to model the propagation of sound within an environment, taking into consideration both specular and diffuse reflections, refraction, absorption and most notably diffraction, in an efficient manner, allowing sonel mapping to be used to model complex interactive virtual environments. Work with respect to this goal is ongoing and although diffraction and refraction have yet to be added, the current system supports specular and diffuse reflections in any combination.

Accounting for Frequency: Following the common approach in architectural acoustics applications [15], the distribution of sound frequency in a given sound source is approximated by considering the center frequency of a fixed number of frequency bands ranging from 63Hz to 8kHz. Table 1 provides a summary of the frequency bands used here along with their associated lower f_l , upper f_u and center frequency f_c . Each sonel holds the energy contained in each frequency band and currently each frequency band (center frequency) is considered separately at each stage of the simulation.

3.1: Addressing the Differences Between Light and Sound Waves

Two basic differences between the propagation of light and sound waves that must be addressed by any acoustical modeling method employing visual (light) based techniques are [17, 20]: i) the slower propagation speed of sound and ii) the greater attenuation (damping) of sound by the medium

Bandwidth	f_l (Hz)	f_u (Hz)	f_c (Hz)
1	44	89	63
2	89	177	125
3	177	354	250
4	354	707	500
5	707	1400	1000
6	1400	2800	2000
7	2800	5600	4000
8	5600	11300	8000

Table 1. Bandwidths and center frequencies.

(air).

Accounting for Absorption by the Medium: Assuming planar sound waves, the attenuation of sound energy due to absorption by the air follows an exponential law [11]:

$$E_d = E_o e^{-md} \quad (1)$$

where E_o is the energy of the sound at the original position, E_d is the energy after the sound has traveled a distance d and m is the air absorption constant and varies as a function of the conditions of the air itself (e.g., temperature, frequency, humidity and atmospheric pressure). Expressions for the evaluation of m are provided by Bass et al. [2] and a list of values for m for various frequencies and relative humidity values, at constant air temperature of 20°C and normal atmospheric pressure of 10^{-3}m^{-1} is provided by Kuttruff [11].

Accounting for the Finite Propagation Speed of Sound: Each sonel contains information to describe the total distance it has traveled. During each interaction (intersection) between a sonel and a position x on a surface S , the distance between point x and the point x' from which the sonel was last emitted/reflected from is determined and this is added to the accumulated distance field of the sonel (d_{sonel}). When required by the simulation (e.g., when the sonel reaches a receiver), the total time t_{sonel} between the emission of the sonel by a sound source and the time it reaches the receiver can be determined by dividing the distance traveled by the speed of sound v_s (e.g., $t_{sonel} = d_{sonel}/v_s$).

3.2: Stage One: Sonel Tracing

In the first stage of the sonel mapping method, the sonel maps are constructed (“populated”). The sonel map is a “global” structure used in the second stage (rendering stage) to determine the sound energy reaching a receiver which has been reflected diffusely at least once independent of the receiver’s position or orientation. From each sound source, a pre-determined (user specified) number of sonels are emitted and traced through the environment. When the sonels encounter a diffuse surface, the information contained in each sonel is updated (this process is described below) and the sonel is stored in the sonel map.

Sound Sources - Emitting the Sonels: Sonels are generated based on the distribution of sound energy in different direction at each source. Currently, omni-directional point sources are used where the sonels are emitted uniformly in all directions. Each sound source generates N_{sonel} sonels from the energy distribution function of the sound source. Accuracy of the estimation increases as more sonels are emitted however, increasing the number of emitted sonels leads to a corresponding increase in computation time. The total power of each source is divided equally amongst each of the sonels emitted from it. Given an omni-directional sound source with a power level of L_s dB, the energy E_o of each sonel when emitted from the source is determined as:

$$E_o = \frac{10^{L/10}}{N_{sonel}} \times 10^{-12} \quad (2)$$

The energy of each sonel is divided equally amongst each frequency band. As sonels propagate through the environment they may interact with a surface. Sonels that do not interact with a surface are lost.

Upon encountering a surface, three types of interaction (specular and diffuse reflection and absorption) will occur simultaneously provided the percentage of the sonel's energy has not decreased below a user defined energy discontinuity percentage (EDP). The EDP represents the percentage of the original (sonel) energy which must be lost before the sonel is terminated (e.g., not reflected any further) [4]. The incident sonel is reflected both specularly and diffusely and the energy carried by each of the reflected sonels is determined as follows:

$$\alpha + \delta(1 - \alpha) + (1 - \delta)(1 - \alpha) = 1 \quad (3)$$

where α is the incident surface absorption coefficient indicating the fraction of sound energy absorbed by the surface, δ is the incident surface diffuse reflection coefficient indicating the fraction of sound energy reflected diffusely and $(1 - \delta)(1 - \alpha)$ represents the amount of energy reflected specularly. Hence, at each point of incidence (provided $\alpha < 1$ and $\delta < 1$), two "new" sonels are created; one is reflected specularly and the other diffusely.

Specular Reflection: When a sonel is reflected specularly, the sonel is reflected assuming ideal specular reflection whereby the angle of reflection is equal to the angle of incidence. Prior to reflecting the sonel, its relevant parameters are updated to account for the intersection with the surface at point x . This includes adding the distance between the last intersection point and the current intersection point to the total distance traveled by the sonel, updating the current point of intersection and surface normal.

Diffuse Reflection: When a sonel is reflected diffusely (e.g., $\delta > 0$), the incident sonel is updated (e.g., position of interaction on the surface x , surface normal, distance traveled, energy reduced due to absorption etc.) and the sonel

is stored in the sonel map. A new sonel is then generated and reflected diffusely from this point on the surface. The direction (θ, ϕ) of reflection for this new sonel is determined by choosing a random direction in the hemisphere centered about point x . For a perfectly diffuse (Lambertian) surface, directions are chosen uniformly over the hemisphere centered above point x .

3.3: Stage Two: Acoustic Rendering

After construction of the sonel map, rendering of the acoustic environment takes place. In the rendering stage, the room impulse response is estimated through the use of the previously constructed sonel map coupled with acoustic distribution ray tracing. The impulse response is estimated by emitting acoustic rays from each receiver and tracing them through the scene, recording their interaction with any objects/surfaces. The impulse response (echogram) describes the distribution of sound energy over time. Time is discretized and the spacing between "time steps" or "bins" is denoted by p_s . As with the sonels emitted from sound sources in stage one, the rays emitted from the receiver can encounter either a specular or diffuse surface. Greater detail regarding each of these two interactions are provided below.

Diffuse Reflection: When the ray intersects a diffuse surface at point x , the sonel map is used to provide an estimate of the sound energy leaving point x and arriving at the receiver. The estimate is made using a modified form of the *density estimation* algorithm described by Jensen [8]. A maximum number of sonels n_{max} in the sonel map closest to the intersection point x are found by searching the sonel map for all sonels within a pre-defined distance d_s of x (the actual number found n_{actual} may be less than n_{max}). In reality, not all sonels matching this criteria will necessarily reach point x' , however, currently, it is assumed all sonels do (future versions will consider including some form of distribution function that describes the distribution of energy reaching point x' from point x). The energy of each sonel (each frequency band) is scaled by $1/n_{actual}$ and further scaled to account for attenuation by the air. Prior to scaling for attenuation by the air however, the distance between point x' and point x is calculated and this is added to the total distance field of the sonel to account for the path between the two points. The scaled energy of each of the n_{actual} sonels is then added to the appropriate "bin" b_i of the accumulating impulse response using Equation 4 given below and the ray is terminated.

$$b_i = \left[((t_{sonel} + t_{ray}) \times \frac{1}{p_s}) + 0.5 \right] \quad (4)$$

where t_{ray} is the time taken for the ray emitted by the receiver to reach point x and t_{sonel} is obtained from the sonel itself (see Section 3.1).

Surface	Material	α (2kHz)	α (4kHz)
Floor	Wood (on joists)	0.15	0.11
Ceiling	Plaster (smooth finish)	0.14	0.10
Walls	3/8" Plywood panel	0.28	0.22

Table 2. Surface absorption coefficients.

Specular Reflection: Specular reflections are handled using the approach described for specular reflections in stage one. However, in contrast to stage one, when a sound ray encounters a sound source (acting as a receiver), its energy is scaled to account for attenuation of the medium and distance. As with diffuse reflections, the appropriate impulse response “bin” is determined as follows:

$$b_i = \left\lfloor \left(t_{ray} \times \frac{1}{p_s} \right) + 0.5 \right\rfloor \quad (5)$$

The scaled energy is added to it. The ray is then terminated (e.g., it is not reflected off of the sound source).

4: RESULTS

To demonstrate the ability of the sonel mapping algorithm to model the acoustics of an environment, the reverberation time (RT) for a simple, “box-like” enclosure was estimated by the system for several sound source/receiver configurations (two frequency bands, with center frequencies of 2kHz and 4kHz were considered for this demonstration). The difference between the estimated and theoretical values predicted by Sabine’s formula [15] is used to provide a measure of system accuracy. The dimensions of the room were 10m \times 9m \times 8m. The position (x, y, z coordinates, in meters) of the single omni-directional sound source were (9.0, 8.0, 7.0), while the coordinates of the four receivers were (4.0, 4.5, 4.0), (2.0, 5.5, 7.0), (3.0, 1.0, 3.0) and (6.0, 6.0, 4.0). The surfaces of the room (four walls, ceiling and floor) were assigned frequency dependent absorption coefficient values α corresponding to particular materials as given in [15] (e.g., a wooden floor on joists, smooth plaster ceiling and each of the remaining four walls 3/8” thick plywood) and listed in Table 2.

As assumed in Sabine’s formulation for reverberation time, in this test all reflections were diffuse (e.g., there were no specular reflections). The diffuse reflection coefficient of surface i (δ_i) was obtained as follows:

$$d_i = 1 - \alpha_i \quad (6)$$

where α_i is the absorption coefficient of surface i . The algorithmic parameters (as described in Section 3) used for this test are summarized in Table 3.

Reverberation times were estimated by computing a linear regression on the -5 to -35 dB portion of the decay curve [12]. The decay curve itself was obtained using Schroeder’s backwards integration method [19].

Parameter	Value
Receiver Radius	0.12m
Source Power	90dB
EDP	99.999999
Echogram bin spacing (p_s)	0.0001s
Number of Sonels (N_{sonel})	100,000
d_s	0.1
n_{max}	10

Table 3. Sonel mapping algorithmic parameters.

Table 4 lists the percent difference $\%dif$ between the predicted (actual) reverberation time $RT_{predicted}$ as predicted by Sabine’s formula and the reverberation time as estimated by the system $RT_{estimated}$, calculated as follows:

$$\%dif = \left| \frac{RT_{predicted} - RT_{estimated}}{RT_{predicted}} \right| \quad (7)$$

As shown in Table 4, the percentage difference between the estimated and predicted reverberation times is very small for each of the receiver positions and for both frequency bands. Although the estimated values are very close to the predicted values, this was obtained by setting the energy discontinuity percentage (EDP) to a very high value of almost 100% when in reality, the EDP is typically set between 90 and 99% [24]. Setting the EDP to such a high value ensures the reverberation decay is linear and hence the linear regression used to estimate the reverberation time provides an accurate measure [24].

5: SUMMARY

This paper presented a preliminary version of the sonel mapping acoustic modeling method. The goal of sonel mapping is to model the acoustics of an environment, taking into account the various acoustical phenomena occurring as a sound propagates and interacts with objects/surfaces in the environment, in an efficient manner thereby allowing it to be used in interactive virtual environments. Currently, the method accounts for specular and diffuse reflections in addition to absorption as a sound propagates from the sound source to the receiver. Preliminary results based on a comparison between the estimated and predicted reverberation times indicate the method accurately estimates the decay of diffusely reflected sound. This work is ongoing and future versions will include modeling of refraction and diffraction effects in order to fully capture the interactions between a propagating sound and objects/surfaces in the environment. More realistic sound source sonel distribution functions are being pursued which take into account frequency dependent source directivity. In addition, the use of a Russian Roulette strategy [22] is being investigated to decrease the computational requirements of the sonel mapping approach.

Position	RT _{predicted} (2kHz)	RT _{estimated} (2kHz)	%dif	RT _{predicted} (4kHz)	RT _{estimated} (4kHz)	%dif
4.0, 4.5, 4.0	2.42s	2.45s	1.24	1.80s	1.81s	0.56
2.0, 5.5, 7.0	2.42s	2.38s	1.65	1.80s	1.71s	5.00
3.0, 1.0, 3.0	2.42s	2.40s	0.83	1.80s	1.72s	4.44
6.0, 6.0, 4.0	2.42s	2.54s	5.00	1.80s	1.84s	2.22

Table 4. Comparison between estimated and predicted reverberation time for four receiver positions.

Acknowledgments: The authors wish to thank Professor Wolfgang Stürzlinger for his valuable input and for his advice on photon mapping. The financial support of the Natural Sciences and Engineering Research Council of Canada (NSERC), the Ontario Graduate Scholarships in Science and Technology (OGSST), CRESTech and a York University President’s Dissertation Scholarship to B. Kapralos is gratefully acknowledged.

References

- [1] J. B. Allen and D. A. Berkley. Image method for efficiently simulating small-room acoustics. *Journal of the Acoustical Society of America*, 65(4):943–950, 1979.
- [2] H. E. Bass, L. C. Sutherland, and A. J. Zuckerwar. Atmospheric absorption of sound: Update. *Journal of the Acoustical Society of America*, 88(4):2019–2021, 1990.
- [3] J. Blauert. *The Psychophysics of Human Sound Localization*. MIT Press, Cambridge, MA, USA, revised edition, 1996.
- [4] S. M. Dance and B. M. Shield. Modelling of sound fields in enclosed spaces with absorbent room surfaces. Part i: Performance spaces. *Applied Acoustics*, 58:1–18, 1999.
- [5] T. Funkhouser, N. Tsingos, I. Carlbom, G. Elko, M. Sondhi, J. E. West, G. Pingali, P. Min, and A. Ngan. A beam tracing method for interactive architectural acoustics. *Journal of the Acoustical Society of America*, 115(2):739–756, 2004.
- [6] T. Funkhouser, N. Tsingos, and J.M. Jot. Survey of methods for modeling sound propagation in interactive virtual environment systems. *Presence*, 2004. To appear.
- [7] M. Hodgson. Evidence of diffuse surface reflections in rooms. *Journal of the Acoustical Society of America*, 89:765–771, 1991.
- [8] H. W. Jensen. *Realistic Image Synthesis Using Photon Mapping*. A. K. Peters, Natick, MA, USA, 2001.
- [9] M. Kleiner, D. I. Dalenback, and P. Svensson. Auralization - an overview. *Journal of the Audio Engineering Society*, 41(11):861–875, 1993.
- [10] A. Krokstad, S. Strom, and S. Sorsdal. Calculating the acoustical room response by the use of a ray tracing technique. *Journal of Sound and Vibration*, 8:118–125, 1968.
- [11] H. Kuttruff. *Room Acoustics*. Spon Press, London, England, fourth edition, 2000.
- [12] Y. W. Lam. A comparison of three different diffuse reflection modeling methods used in room acoustic computer models. *Journal of the Acoustical Society of America*, 100(4):2181–2192, 1996.
- [13] B. L. Dalenbäck. Room acoustic prediction based on a unified treatment of diffuse and specular reflection. *Journal of the Acoustical Society of America*, 100(2):899–909, 1996.
- [14] B. Dalenböck. A macroscopic view of diffuse reflection. *Journal of the Audio Engineering Society*, 42(10):793–806, 1994.
- [15] M. Mehta, J. Johnson, and J. Rocafort. *Architectural Acoustics Principles and Design*. Prentice Hall, Inc., Upper Saddle River, NJ, USA, 1999.
- [16] E. Nosal, M. Hodgson, and I. Ashdown. Improved algorithms and methods for room sound-field prediction by acoustical radiosity in arbitrary polyhedral rooms. *Journal of the Acoustical Society of America*, 116(2):970980, 2004.
- [17] R. Rabenstein, O. Schips, and A. Stenger. Acoustic rendering of buildings. In *Proceedings of the 5th International Conference on Building Simulation*, Prague, Czech Republic, September 8-10 1997.
- [18] L. Savioja. *Modeling Techniques for Virtual Acoustics*. PhD thesis, Helsinki University of Technology, Telecommunications Software and Multimedia Laboratory, Helsinki, Finland, 1999.
- [19] M. R. Schroeder. New method for measuring reverberation time. *Journal of the Acoustical Society of America*, 37:409–412, 1965.
- [20] J. Shi, A. Zhang, J. Encarnação, and M. Göbel. A modified radiosity algorithm for integrated visual and auditory rendering. *Computers and Graphics*, 17(6):633–642, 1993.
- [21] R. D. Shilling and B. Shinn-Cunningham. Virtual auditory displays. In K. Stanney, editor, *Handbook of Virtual Environment Technology*, pages 65–92. Lawrence Erlbaum Associates, Mahwah, NJ, USA, 2002.
- [22] J. Spanier and E. Gelbard. *Monte Carlo Principles and Neutron Transport Problems*. Addison-Wesley, Reading, MA USA, 1969.
- [23] R. R. Torres, P. Svensson, and M. Kleiner. Computation of edge diffraction for more accurate room acoustics auralization. *Journal of the Acoustical Society of America*, 109(2):600–610, 2001.
- [24] L. N. Yang and B. M. Shield. Development of a ray tracing computer model for the prediction of the sound field in long enclosures. *Journal of Sound and Vibration*, 229(1):133–146, 2000.